JOURNAL OF Materials CHEMISTRY

Thermally induced segregation of SnO_2 nanoclusters in Sn-doped silica glasses from oversaturated Sn-doped silica xerogels

Norberto Chiodini,* Franco Meinardi, Franca Morazzoni, Jin Padovani, Alberto Paleari, Roberto Scotti and Giorgio Spinolo

Istituto Nazionale Fisica della Materia - Dipartimento di Scienza dei Materiali, Università di Milano-Bicocca, via Cozzi 53, 20125 Milano, Italy

Received 29th August 2000, Accepted 1st December 2000
First published as an Advance Article on the web 24th January 2001

Silica glasses with substitutional Sn-doping or with dispersion of SnO_2 nanoclusters were prepared by the sol–gel method. The occurrence of SnO_2 clustering was investigated by optical absorption, Raman scattering and electron paramagnetic resonance spectroscopies, varying both the tin concentration and the densification temperature of Sn-doped silica xerogels. The 3.7 eV absorption edge of SnO_2 and the A_{1g} Raman mode at 630 cm^{-1} of the SnO_2 phonon spectrum were used to assess the presence of SnO_2 nanoclusters; the yield of X-ray induced paramagnetic E′ Sn centres was monitored to probe the variation in the amount of substitutional Sn centres. The results indicate that the clustering of SnO_2 becomes effective for Sn concentrations $\geqslant 0.8$ mol% and it is competitive with the substitutional doping in xerogels densified at $T \geqslant 900$ °C. No evidence of pre-existent clustering was observed in xerogels densified at lower temperatures in the investigated doping range.

Introduction

It is known that Sn-doping of silica that leads to substitutional introduction of Sn in the SiO_2 network is not easily achievable by conventional synthesis through chemical vapour deposition due to the easy volatilisation of SnO_2.[1] We recently obtained silica glasses with relatively high concentrations of substitutional Sn, up to 0.4 mol% (mol = $SnO_2/(SnO_2+SiO_2)$ molar ratio), by the sol–gel method.[2,3] We also found that the same process can give rise to materials with dispersed SnO_2 nanoclusters when the Sn doping level of xerogels is above 0.8 mol%.[2] Both kinds of materials are technologically interesting for applications in optoelectronics: substitutionally Sn-doped silica is highly photosensitive to UV radiation[1,4] and may be used in optical fibre devices based on Bragg grating technology,[4,5] whereas the second type of material, resembling typical glass ceramics, may be a good candidate for third-order, non-linear optical applications.[6] In order to tune and possibly improve these properties it is important to increase the substitutional Sn-doping level, on one hand, and to control the dimensions and size distribution of the tin oxide clusters, on the other hand. In both cases, the main questions are: is the cluster formation driven by the sol–gel reaction, inclusive of the type and concentration of the metal precursors or is it dependent on the thermal treatment of the xerogels?

In this work Sn-doped silica xerogels with different tin concentrations underwent densification at different temperatures. UV absorption spectroscopy, Raman scattering and electron paramagnetic resonance investigations allowed investigation of the dependence of tin oxide clustering on the Sn-doping content and on the temperature of the xerogel densification.

Experimental

We produced SiO_2 xerogels containing 0.04, 0.2, 0.4, 0.8, 1.2, 1.6, 2.4, and 3.2 mol% of SnO_2 by simultaneous hydrolysis and cogelation of metal precursors, tetraethoxysilane (TEOS) and dibutyltin diacetate (DBTDA), as reported elsewhere.[2] A set of samples covering all the SnO_2 concentrations reported above were densified slowly, increasing the temperature up to 1050 °C, by the same thermal program reported in ref. 2. Complete densification was obtained without sample fracture.

A second set of samples with 0.04, 0.4 and 1.6 mol% of SnO_2 (SnO_2 contents that, by densification up to 1050 °C, give glasses containing substitutional tin in the first two cases and SnO_2 clusters in the latter case) were prepared following a different densification program. Three groups of 10 xerogel samples, with 0.04, 0.4 and 1.6 mol% of tin, underwent the same thermal treatment as in ref. 2 up to 700 °C, but in a pure O_2 atmosphere. After this temperature the thermal treatment consisted of a steep ramp (90 °C h^{-1}) in pure O_2 up to a final temperature which ranged from 700 to 1150 °C, with steps of 50 °C. Each individual sample was kept for 24 hours at the final temperature before being taken out of the oven.

The samples were studied by the micro-Raman technique using a Dilor Labram machine and by UV–Vis spectroscopy using a Varian Cary 50 spectrophotometer and, for small samples, a Perkin Elmer Lambda 900 double grating spectrophotometer.

EPR spectra were recorded at 25 °C on a Bruker EMX spectrometer operating at about 9.6 GHz. The microwave frequency was accurately read with an HP 53131A frequency counter and the g values were standardised by reference to α,α'-diphenyl-β-picrylhydrazyl (DPPH) with $g = 2.0036$. Before EPR measurements the samples were irradiated at 25 °C by means of an X-ray tube (W target, 32 keV, 20 mA) at a dose of 2×10^4 Gy.

Results

Optical absorption spectra of silica glasses, doped with different SnO_2 contents and densified at 1050 °C are reported in Fig. 1. Two clearly distinct groups of samples may be identified according to their absorption features: a) samples with $SnO_2 \geqslant 0.8$ mol%, where the UV spectrum shows an absorption edge at about 3.6 eV, corresponding to an SnO_2 band-to-band transition;[7] b) samples with $SnO_2 \leqslant 0.4$ mol%, where no evidence of the SnO_2 gap transition arises from the spectrum. At higher energy (about 6 eV) the tail of a strong absorption extending in the VUV is observed, together with a

DOI: 10.1039/b006999j

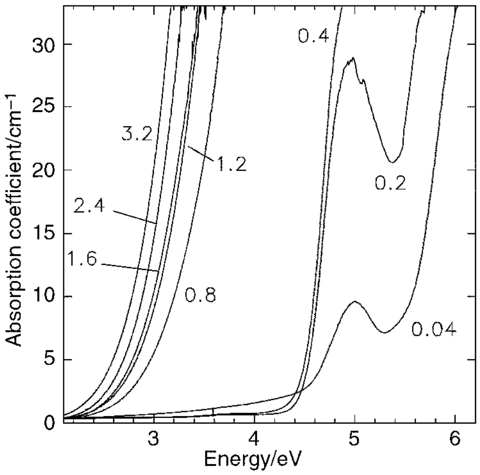

Fig. 1 UV absorption spectra of sol–gel Sn-doped silica samples with different Sn content (mol% values are indicated) after complete thermal treatment at 1050 °C.

very pronounced shoulder at 4.9 eV. The first one is typical of doped silica glasses,[8,9] the other is similar to that observed in Ge-doped silica at about the same energy (5.1 eV)[3,10] and is associated with doping-induced oxygen deficiency.

Fig. 2 reports the UV spectra of xerogels at two dopant concentrations, 0.4 and 1.6 mol% of SnO_2, densified at different temperatures from 700 to 1150 °C with steps of 50 °C (spectra of 0.04 mol% doped samples appear quite similar to that of pure synthetic silica, without any structure below 6 eV). The spectra of the 0.4 mol% doped samples (Fig. 2A) show a strong absorption at about 6 eV, typical of doped silica glasses,[8,9] but with a small shift in energy at densification temperatures >950 °C. At variance with the 0.4 mol% sample reported in Fig. 1, the absorption at 4.9 eV is not observed, because treatment in pure oxygen prevented the formation of oxygen-deficient defects. The spectra of the 1.6 mol% doped samples (Fig. 2B) show the absorption edge of SnO_2 after treatment at temperatures higher than 900 °C; at lower temperatures they are not dissimilar from the 0.4 mol% samples. The inset of Fig. 2 shows the change in spectral position of the absorption curves (taking 50 cm^{-1} as the reference value for the absorption coefficient) for the two groups of samples as a function of the densification temperature: the SnO_2 gap becomes evident in more concentrated samples above 900 °C and indicates the presence of tin clustering effects. The small energy shift in 0.4 mol% samples will not be discussed further.

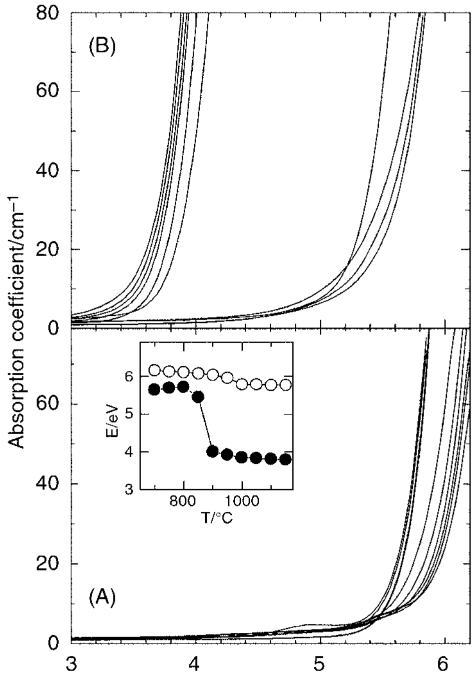

Fig. 2 UV absorption spectra of A) 0.4 mol% and B) 1.6 mol% Sn-doped silica samples produced at different temperatures. For easy identification of the curves, in the inset the energies where the curves take the absorption value of 50 cm^{-1} are reported as a function of the final treatment temperature of the 0.4 mol% sample (open circles), 1.6 mol% sample (filled circles).

Further indication of the occurrence of tin oxide segregation comes from the Raman measurements (see Fig. 3). A 3.2 mol% tin-doped sample, treated above 900 °C, shows a narrow peak at 630 cm^{-1} due to the A_{1g} mode of SnO_2, as well as other less intense SnO_2 features. The peak intensity progressively increases with the treatment temperature. The same sample, treated at $T \leq 900$ °C does not show a peak at 630 cm^{-1}, above the detection limit of the instrument. The 0.4 mol% tin-doped sample does not show a peak at 630 cm^{-1}, regardless of the densification temperature.

The embedding of Sn in substitutional positions for Si in the SiO_2 network was investigated by EPR by monitoring the concentration of paramagnetic E′ Sn centres produced at a given X-ray irradiation dose. The E′ Sn centres consist of an unpaired electron located in the sp^3 orbital of a three-fold coordinated Sn,[11] *i.e.* they are Sn variants of the well known E′ Si centres[12] and can be rightly considered the fingerprint of tin atom substitution for silicon. The number of E′ Sn centres depends on the defect creation yield (which increases by increasing the network density for a given X-ray dose[13]) and on the fraction of Sn atoms in substitutional sites (not belonging to SnO_2 clusters). The representative EPR spectrum of an irradiated Sn-doped sample is reported in Fig. 4. Deconvolution and fitting of the E′ Sn EPR spectrum, in the range 345–350 mT, was reported in a previous paper.[11] It was shown that two E′ Sn variants having different symmetry contribute to the spectrum: the axial variant with $g_{\parallel}=1.994$, $g_{\perp}=1.977$ and the rhombic variant with $g_1=1.994$, $g_2=1.986$, $g_3=1.975$.[11] In fact the shape of E′-like signals depends on the local symmetry of the defect structure, and the axial symmetry of the sp^3 wavefunction may be distorted by non-isotropic surroundings.[11] The relative change in the rhombic contribution to the E′ Sn signal may be estimated from the ratio between the amplitude of the signal at $g_2=1.986$ (B segment in Fig. 4, peculiar to the orthorhombic signal) and the amplitude of the whole signal (A segment in Fig. 4, associated with $g=1.994$ common to both variants). The B : A ratio for 0.04, 0.4 and 1.6 mol% doped samples (inset of Fig. 4) varies with the densification temperature and shows an increasing trend in all

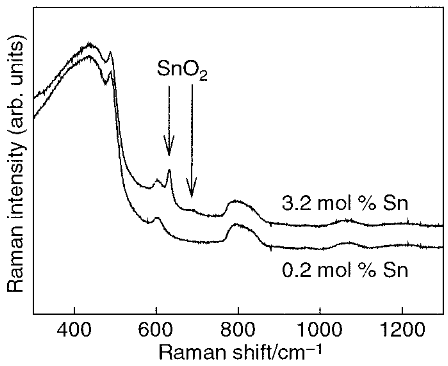

Fig. 3 Raman scattering spectrum of a representative Sn-doped sol–gel silica sample (densified at 1050 °C) where SnO_2 clustering occurs, compared with a non-clustered sample (doping levels are shown). Features due to cassiterite vibrational modes are indicated.

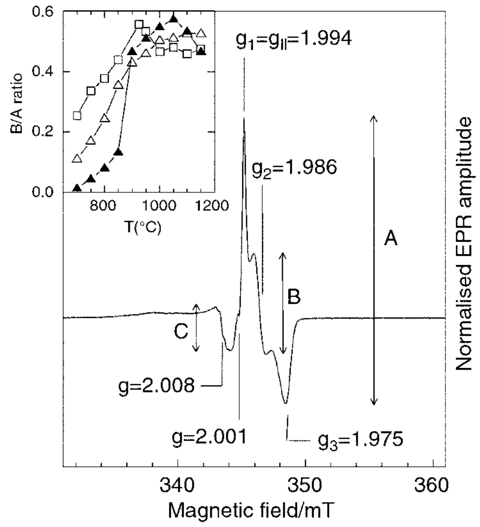

Fig. 4 Representative EPR spectrum of an X-ray irradiated Sn-doped silica sample (0.4 mol% Sn, treated at 850 °C). Spectral positions and *g*-values of the signals due to E′ Si, E′ Sn and NBOH centres are indicated (see text). In the inset the amplitude of the g_2 component of the orthorhombic variant of the E′ Sn signal (normalised to the full amplitude of the whole signal) is reported for the 0.04 (open squares), 0.4 (open triangles) and 1.6 mol% (filled triangles) Sn-doped samples.

cases. Other signals were observed due to non-bridging-oxygen hole (NBOH) centres (signal at about $g=2.01$,[14] C segment in Fig. 4) and to intrinsic E′ Si centres (narrow signal at about $g=2.001$).

The relative concentration of E′ Sn centres (resulting from double integration of the whole E′ Sn signal comprising orthorhombic and axial variants), in 0.04, 0.4 and 1.6 mol% doped samples treated at different densification temperatures at a fixed X-ray dose, is shown in Fig. 5A. The E′ Sn concentration increases with the treatment temperature over the range 700 to 850 °C, which is consistent with the expected effect of SiO_2 densification on the E′ centre creation yield.[13] In this temperature range the radiation-induced E′ Sn concentration is higher in the most heavily doped samples. A clear decrease is instead observed by increasing the treatment temperature; this is more pronounced in the 1.6 mol% doped sample where above 900 °C the radiation-induced E′ Sn density falls below that measured in the 0.04 mol% doped sample. Above 1000 °C the E′ Sn creation yield is stable around values differing by more than one order of magnitude, the lowest value being that observed in the 1.6 mol% doped sample where clustering occurs. The lowest relative decrease with respect to the maximum yield is observed in the 0.04 mol% samples. Fig. 5B and 5C show the normalised amplitude ratio of the signal due to NBOH centres or, respectively, to E′ Si centres and that due to the E′ Sn centres in samples densified at different temperatures.

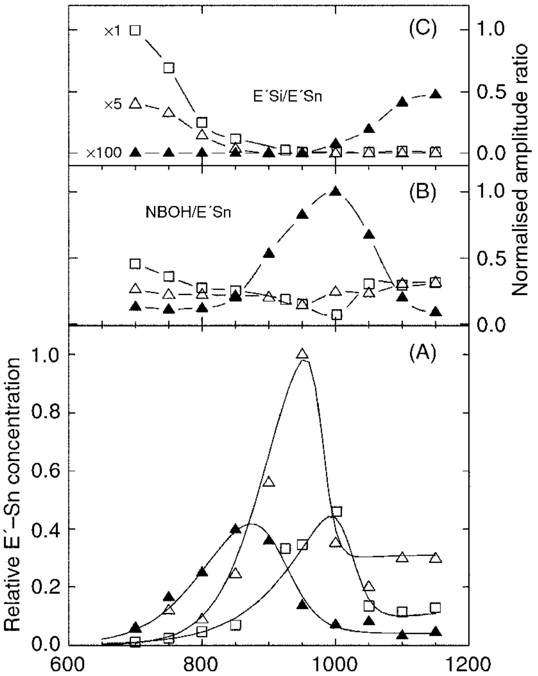

Fig. 5 A) Relative E′ Sn centre concentration at fixed X-ray dose in 0.04 (open squares), 0.4 (open triangles) and 1.6 mol% (filled triangles) Sn-doped samples, estimated by comparison of double integrated EPR first derivative spectra. B) Amplitude ratio between NBOH and E′ Sn signals and C) E′ Si and E′ Sn signals in 0.04 (open squares), 0.4 (open triangles) and 1.6 mol% (filled triangles) Sn-doped sample. (Lines are guides for the eyes.)

Discussion

Three main results can be highlighted. (i) The appearance of the absorption edge at about 3.7 eV (which corresponds well to the SnO_2 band gap[7] and is related to the SnO_2 phase[15] observed in the Raman spectrum of Fig. 3) depends on both the SnO_2 content (Fig. 1) and the treatment temperature of samples (Fig. 2). (ii) The SnO_2 clustering in the 1.6 mol% sample is accompanied by a large decrease in the number of dispersed substitutional Sn centres, as monitored by the trend of EPR active E′ Sn centres, whose number falls below that observed in the 0.04 mol% sample (Fig. 5A). (iii) Even if clustering does not occur (as in the 0.04 and 0.4 mol% samples), a decrease in the E′ Sn creation yield is observed above 1000 °C, but is more evident in highly doped samples (Fig. 5A).

Point (i) indicates that the SnO_2 clustering in Sn-doped silica samples obtained by the described sol–gel method is a thermally activated process. Point (ii) shows that the clustering process is competitive with the Sn presence in regular Si sites. Moreover, the decrease in the substitutional Sn caused by SnO_2 segregation in the 1.6 mol% sample is so large that the number of E′ Sn centres falls well below that observed in the 0.4 mol% tin-doped glass, *i.e.* the most concentrated sample where segregation does not occur. This fact suggests that non-segregated, but rather highly doped, Sn samples (0.4 mol%) may be considered similar to an oversaturated doped system. After clustering the residual E′ Sn content would be related to the solubility level of SnO_2 in silica. Point (iii) suggests that some kind of thermally activated Sn-related process takes place even in samples where there is not formation of the SnO_2 phase, probably reflecting an incipient clustering of Sn sites with a related modification of the Sn site environment. Aggregation of few Sn sites, still in a silica-like structure with tetrahedral coordination, might be associated to the decrease of the E′ Sn creation yield by supposing that this aggregation lowers the number of E′ Sn precursors. The change in the environment of the Sn sites expected from this kind of aggregation is also supported by the change in the spectral shape of the E′ Sn EPR signal. In fact, the predominant symmetry of the E′ Sn centres changes from axial to orthorhombic on continuing with the thermal treatment up to the onset of the clustering process, if any (inset of Fig. 4). A more distorted environment characterises the E′ Sn centres related to the aggregates, whereas a nearly axial defect structure pertains to E′ Sn centres arising from Sn sites well diluted in the silica network. The increase in the axial character observed in samples with SnO_2 clusters may similarly be interpreted as an indication that the residual substitutional Sn sites are well diluted in the silica network, as they are in the low-level doped samples or in samples treated at low temperature.

The creation of NBOH centres in the 0.04 and 0.4 mol% doped samples is correlated with the creation of E′ Sn centres and the amplitude ratio of the related signals is quite constant (Fig. 5B). By contrast, in the 1.6 mol% doped samples, the beginning of the clustering process is accompanied by a clear enhancement of the formation of NBOH centres. In these samples, NBOH centres probably arise from the broken or stressed bonds involved in the change of Sn coordination during the first step of the SnO_2 cluster nucleation. The creation yield of E′ Si centres (Fig. 5C) confirms the competitive formation of E′ Sn and E′ Si defects; in fact, the amplitude of the E′ Si signal, compared to that of the E′ Sn signal, decreases with the temperature when the temperature favours the creation of E′ Sn centres (from 700 to 850 °C). E′ Si defects are undetectable in the treatment range $700 < T < 1000\,°C$, while at $T > 1000\,°C$ they become well evident.

Conclusions

The data show that the described sol–gel method produces Sn-doped silica xerogels that, even at high tin concentrations, are free from SnO_2 segregates. At tin concentrations higher than 0.8 mol% the stability of substitutional Sn (diluted in the silica network) is contrasted by the thermally activated mechanisms that give rise to SnO_2 clustering. Therefore, both the composition of the xerogels and the densification temperature can be suitably controlled in order to obtain silica-based materials with a high level of substitutional Sn-doping or with dispersed SnO_2 clusters.

Acknowledgement

This work was carried out within a National Research Project supported by the Ministero dell'Università e della Ricerca Scientifica e Tecnologica.

References

1 G. Brambilla, A. Pruneri and L. Reekie, *Appl. Phys. Lett.*, 2000, **76**, 807.
2 N. Chiodini, F. Morazzoni, A. Paleari, R. Scotti and G. Spinolo, *J. Mater. Chem.*, 1999, **9**, 2653.
3 N. Chiodini, F. Meinardi, F. Morazzoni, A. Paleari, R. Scotti and D. Di Martino, *J. Non-Cryst. Solids*, 2000, **261**, 1.
4 B. Poumellec and F. Kherbouche, *J. Phys. III*, 1996, **6**, 1595.
5 J. Albert, *MRS Bull.*, 1998, **23**, 36.
6 W. Nie, *Adv. Mater.*, 1993, **5**, 520.
7 J. Robertson, *J. Phys. C: Solid State Phys.*, 1976, **12**, 4767.
8 M. J. Yuen, *Appl. Optics*, 1982, **21**, 136.
9 A. Anedda, C. M. Carbonaro, A. Serpi, N. Chiodini, A. Paleari, R. Scotti, G. Spinolo, G. Brambilla and A. Pruneri, *J. Non-Cryst. Solids*, in the press.
10 L. Skuja, *J. Non-Cryst. Solids*, 1992, **149**, 77.
11 N. Chiodini, F. Meinardi, F. Morazzoni, A. Paleari, R. Scotti and G. Spinolo, *Phys. Rev. B: Condens. Matter Mater. Phys.*, 1998, **58**, 9615.
12 D. L. Griscom, *J. Ceram. Soc. Jpn.*, 1991, **99**, 899.
13 R. A. B. Devine and J. Arndt, *Phys. Rev. B: Condens. Matter Mater. Phys.*, 1989, **39**, 5132.
14 D. L. Griscom and E. J. Friebele, *Phys. Rev. B: Condens. Matter Mater. Phys.*, 1981, **24**, 4896.
15 L. Abello, B. Bochu, A. Gaskov, S. Koudryavtseva, G. Lucazeau and M. Roumyantseva, *J. Solid State Chem.*, 1998, **135**, 78.